



KAMAX INNOVATIVE SYSTEM

XPolar® Technology: Theory and Applications

February 3, 2020



CONTENTS

1	Introduction: Light polarization in Nature	2
2	XPolar technology	3
3	Application: study of skin aging	5
3.1	Collagen and light polarization	5
3.2	application: collagen glycation	6
3.3	Conclusion	8
4	Application: hair oxidation study	8
4.1	Keratin and light polarization	8
4.2	Application: assessment of anti-oxidation active product	9
4.3	Conclusion	12
5	Glossary	12
5.1	Anisotropy	12
5.2	Birefringence	13
5.3	Crossed polarizers microscopy	14
5.4	Electromagnetic wave	14
5.5	K_{\max}	14
5.6	Polarimetry	15
5.7	Refractive index	15
5.8	State of polarization	15
5.9	Wavelength	17

FOREWORD

A glossary intended to facilitate the understanding of the XPolar technology is in section 5, with a general description of the main subjects introduced. One should refer for example to the book "*Polarized Light*" [1] for a more detailed description.

1 INTRODUCTION: LIGHT POLARIZATION IN NATURE

We focus on the electromagnetic description of light. **Polarization** of light describes one of its properties, as its intensity or its **wavelength** (color). However, the human eye is not sensitive to the **polarization**.

Many insects are sensitive to **polarization**. For example, bees (*Apis*) [2] or the desert ant (*Cataglyphis bicolor*) [3], use the **polarization** of light to navigate, the sky **polarization** being variable with the direction of observation. Besides, the Mantis-shrimp (Stomatopoda), which has one of the most complex visual system among animals, is sensitive

to the [polarization](#) [4][5] and uses it for communication, as it is also capable to emit polarized light.

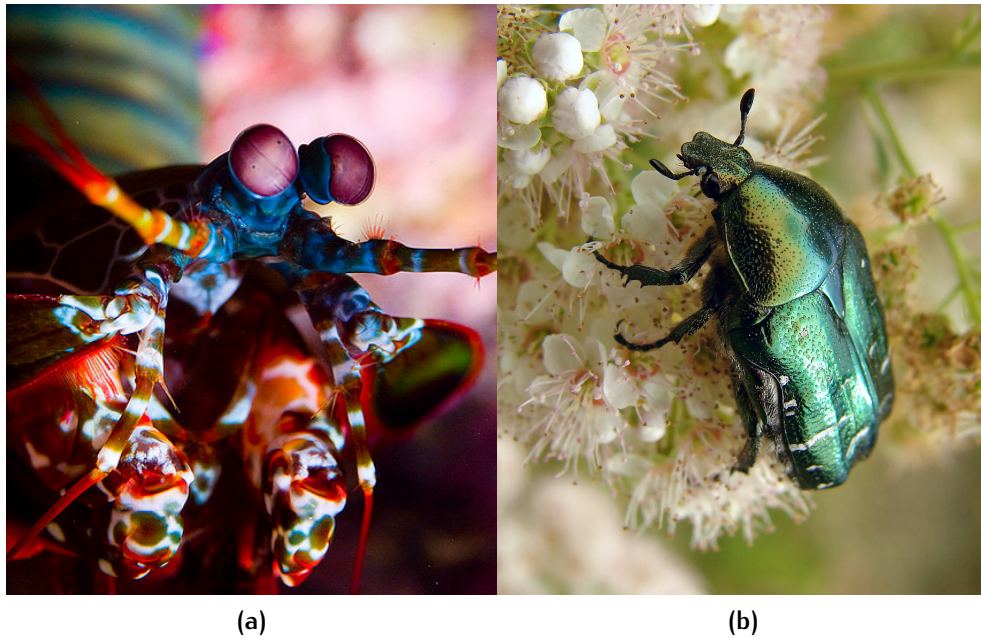


Figure 1: (a) Mantis-shrimp[†] (Stomatopoda), which is sensitive to polarized light. (b) Rose chafer (*Cetonia aurata*), which exocuticle reflects circularly polarized light.

Other animals have developed structures on their cuticle that reflect polarized light, as some beetles, for example *Chrysina gloriosa* [6], *Anomala dubia*, *Anomala vitis*, *Cetonia aurata* and *Potosia cuprea* [7]. The fact that they reflect polarized light suggest that they are also sensitive to it [8].

2 XPOLAR TECHNOLOGY

The XPolar technology is an imaging device integrated in a microscope, allowing to observe and measure the polarimetric properties of the studied samples. More precisely, XPolar technology gives information on the [birefringence](#) of the sample.

The optical apparatus is schematized in Fig. 2: the laser source emit a polarized light passing through a circulator (C), then through a [polarization](#) scrambler (Br) which modifies its [state of polarization](#), and is finally focused on a sample (S) by a lens (O). The reflected [wave](#) is collected by the lens (O), contra-propagates through the scrambler

[†]CC BY-SA Nazir A.

(Br), and is then split by the circulator (C) into two components orthogonally polarized. The light intensity of these two components is measured by two photodiodes, respectively (A) and (B). The light intensity measured by the photodiode (A) is called I_{\perp} , and I_{\parallel} the light intensity measured by the photodiode (B), \perp and \parallel describing the orthogonal states of polarimetric projection.

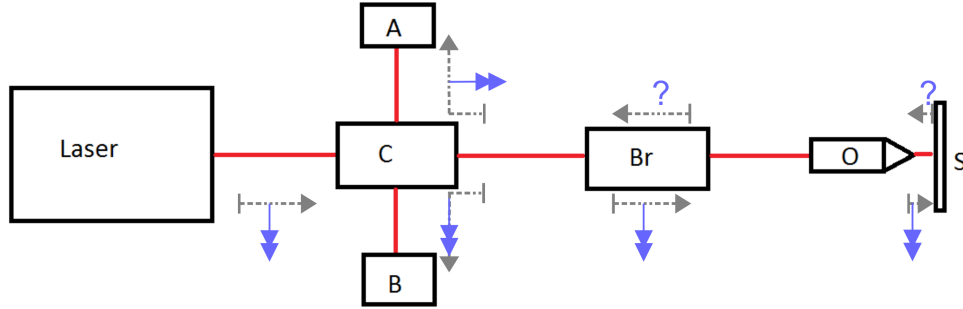


Figure 2: Schematized view of the optical apparatus. It is composed of a laser source, a circulator (C), a **polarization** scrambler (Br), a sample (S), a lens (O), two photodiodes (A) and (B). Gray: direction of light propagation. Blue: schematic representation of the light **state of polarization**.

The incident **state of polarization** is set by the **polarization** scrambler. This state changes randomly during a measurement sequence and can take any value among all possible **polarization states**. The two intensity levels I_{\perp}^k and I_{\parallel}^k measured for one incident **state of polarization** k are stored by the computer. This operation is repeated with N **states of polarization**, thus N measured values I_{\perp} and I_{\parallel} are stored by the computer. From these measurements, a parameter called K_{\max} [9] is computed :

$$K_{\max} = \max_{k=1:N} \left\{ \frac{I_{\perp}^k}{I_{\parallel}^k + I_{\perp}^k} \right\}$$

That (scalar) measurement is repeated on 800×600 points on the sample, by moving the lens focal point in the sample plane, which forms an (matrix) image.

The K_{\max} parameter gives information on the sample **birefringence** on each point of the image, it can be used to quantitatively characterize the sample and/or to quantify its variations in the field of view.

Illuminating the sample with a large number (N) of different **states of polarization** to obtain one K_{\max} value allows to overcome potential optic axis rotations in the sample plane (see section 5.2 for a description of the optic axis of uniaxial materials). It can be understood

(but it is not strictly equivalent) as a measurement which takes into account all angles of sample rotation between [crossed polarizers](#).

Table 1: [XPolar](#) technical specifications.

Specification	Value
Image size	800×600 pix.
Field of view	200 × 150 μm
Spatial resolution	0.25 × 0.25 μm/pix.
Magnification	400×
Max. sample thickness	150 μm
Wavelength	780 nm
Frames per second	15 Hz
HDR modes	Low, Medium, High
K _{max} resolution	0.01

3 APPLICATION: STUDY OF SKIN AGING

3.1 Collagen and light polarization

Collagens are one kind of structural proteins. Found in the extracellular matrix of animal organisms, they confer mechanical resistance to stretching. Thus they can be found in large quantities in the skin.

Collagen fibers are maintained together by hydrogen bond between the glycin of their proteins. It forms a structure comparable to a crystal lattice, with an [anisotropy](#) that leads to a [polarization](#) modification when light passes through the collagen. Indeed, the light polarized with a state parallel to the fibers will not propagate at the same speed than the light polarized perpendicularly to the fibers. That retardance is described by a property called [birefringence](#), which varies with the quality of the collagen "lattice", and with the collagen thickness crossed by the light.

The light [polarization](#) modification produced by the collagen can be amplified by using a histology stain, for example sirius red [10], the stain producing [polarization](#) modifications when it is fixed on collagen. However, the use of staining is not always mandatory.

Thus, a modification of the collagen quantity or structure will lead to a variation of the measured [birefringence](#) [11].

3.2 application: collagen glycation

Collagen glycation is a natural process, in which a sugar links to a collagen protein, producing residues called AGEs (advanced glycated end products) [12].

With *XPolar* technology, we will measure the polarimetric modifications of collagen during a glycation process. For that purpose, methylglyoxal is used on human skin explants [13].

We will also perform polarimetric measurements on a sample treated with aminoguanidine hydrochloride 1%, an inhibitor of the glycation process. [14].

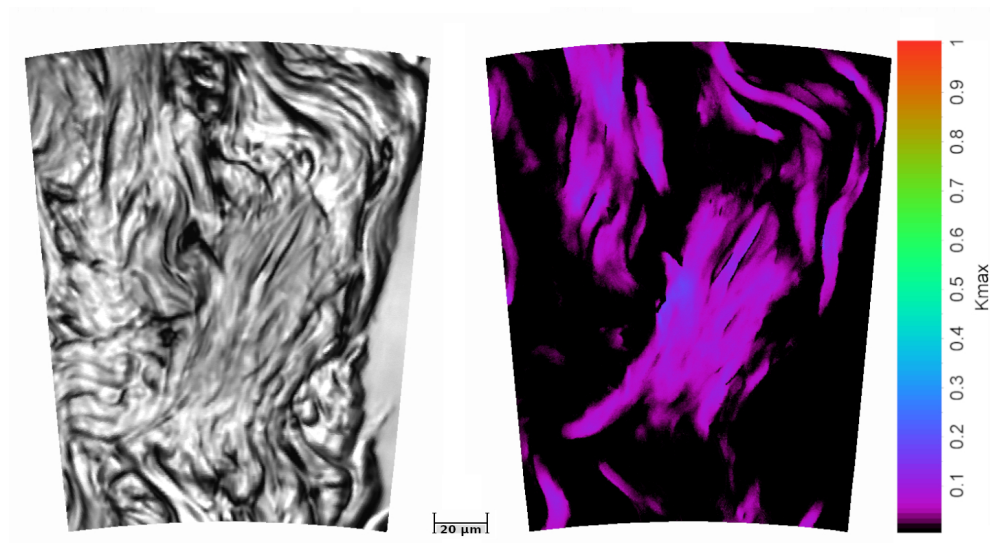


Figure 3: XPolar measurement example, on a skin explant. Left: reflected intensity image. Right: K_{max} value image.

To characterize the polarimetric properties of explants, we measure the reflected K_{max} parameter (see section 5.5 for more details), more precisely we compute the average value of this parameter on the field of view, without taking into account the areas where the polarimetric signal is absent. This parameter is called weighted average and it only depends on the collagen thickness and structure.

An example of K_{max} image is plotted in Fig. 3, which was measured on a 20 μm thick explant without staining. The reflected intensity image is on the left, the K_{max} image is on the right.

We repeat this measurement for various methylglyoxal concentrations (500, 750 and 1000 μM), and we compute the weighted average value. We measure a decrease of the average value of respectively 34

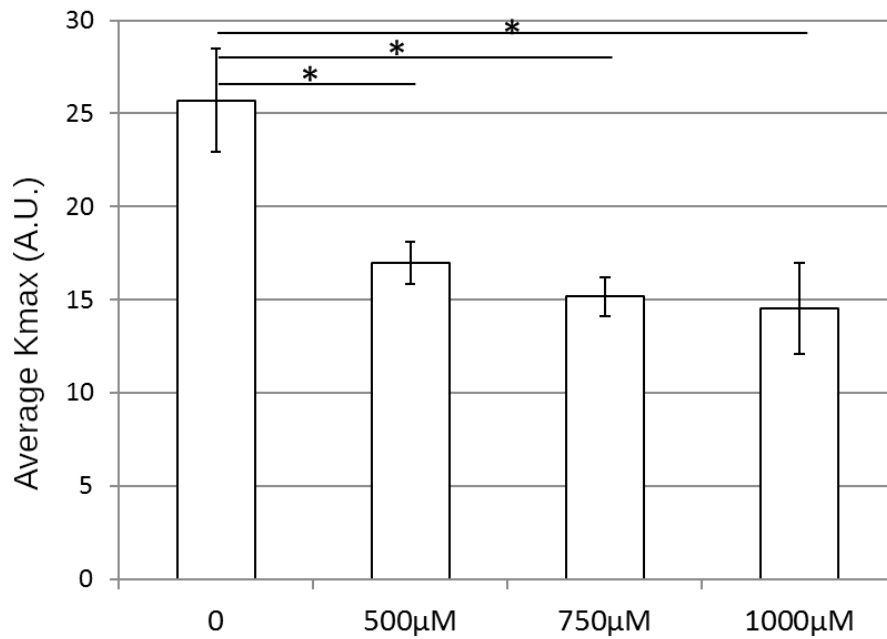


Figure 4: Mean K_{max} value, computed by taking into account only the areas with a non zero value, versus the methylglyoxal concentration applied on the sample. The higher the concentration is (i.e. there is more glycation), the lower the averaged birefringence is.

% ($p < 0.05$), 41 % ($p < 0.01$) and 43 % ($p < 0.01$) versus the methylglyoxal concentration, as plotted in Fig. 4.

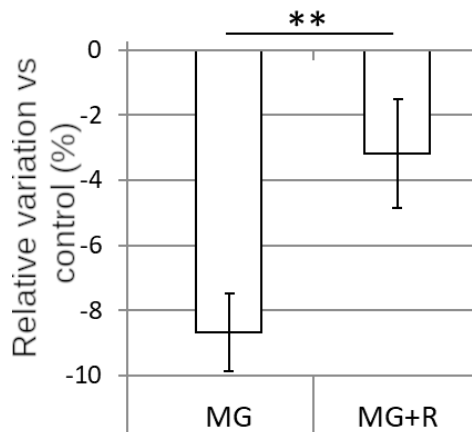


Figure 5: Relative variation respectively to the control sample of the weighted average value, for the sample with only glycation (MG) and the sample which has been treated beforehand with an anti-glycation active product (MG+R).

That measurement is repeated on explants previously treated with anti-glycation active product (aminoguanidine hydrochloride 1%). The results are summarized in Fig. 5, we measure an attenuation of 63 %

($p < 0.05$) of the weighted average decrease after the use of the active product.

3.3 Conclusion

We have demonstrated that the collagen, even without sirius red staining (or other staining), produces a polarimetric signal that can be measured with **XPolar** technology. That property depends on the collagen thickness crossed, and its structural condition.

The XPolar technology is then applied to measure the thickness and structural condition of the collagen before and after an aging process called glycation, we have demonstrated that the method allows to quantitatively assess the glycation process. Besides, we demonstrated that the method can also quantify the efficiency of an anti-glycation active product [11].

Other process can lead to a **birefringence** modification of the skin, for example the use of ceramides to reinforce the stratum corneum.

4 APPLICATION: HAIR OXIDATION STUDY

4.1 Keratin and light polarization

The hair is composed of keratin, a family of fibrous proteins. The α -keratin fibers have a crystalline part [15], bonded by Coulomb forces and hydrophobic interactions. These fibers are also known to have a high concentration of disulfide bridges [16] between the proteins by the cysteine.

That crystalline structure of keratin fibers confers to the hair the ability to modify the **polarization** of light that passes through it, a property which is called birefringence.

Indeed, the light with a **state of polarization** parallel to the keratin fibers will not propagate at the same speed than the light with a **polarization** perpendicular to them. That property is called **birefringence**, it depends on the hair thickness and on the crystalline condition of the keratin. If the keratin is degraded, the hair **birefringence** will decrease. [15].

Hydrogen peroxide (H_2O_2) is known to degrade the melanin and thus it has a bleaching effect. However, it also targets the disulfide bridges by oxidation of the cysteine, producing cysteic acid [17]. That

degradation of the fibers structure leads to a decrease of the hair [birefringence](#), which can be measured with [XPolar](#) technology.

4.2 Application: assessment of anti-oxidation active product

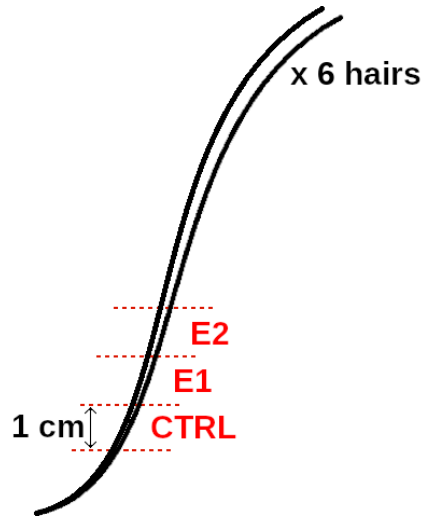


Figure 6: Schematic view of the samples preparation, cut in the same lock of hair.

We perform the following procedure:

- Selection of 6 hairs in one lock.
- Cut 3 contiguous samples, about 1 cm long, as schematized in Fig. 6.
- Antioxidant application during 45 mn on the E2 sample.
- Oxidation of samples E1 and E2 with hydrogen peroxide (6 % H_2O_2) during 45 mn and rinse it with distilled water.
- Dry during 30 mn at $37^\circ C$, then mount the sample between a slide and a cover slip.

An example of slide mounted with 6 hairs is plotted on Fig. 7. We perform 2 XPolar measurements per hair, which gives images as the one represented in Fig. 8. One can notice the K_{max} periodicity in the image at the right: in function of the transverse position in the hair, the K_{max} value increases from black to red, then decreases and increases again, etc. That periodicity can be explained by the fact that the K_{max} value is depending on the material thickness crossed (for more details, see section 5.5), which varies transversely as the hair is roughly a cylinder.

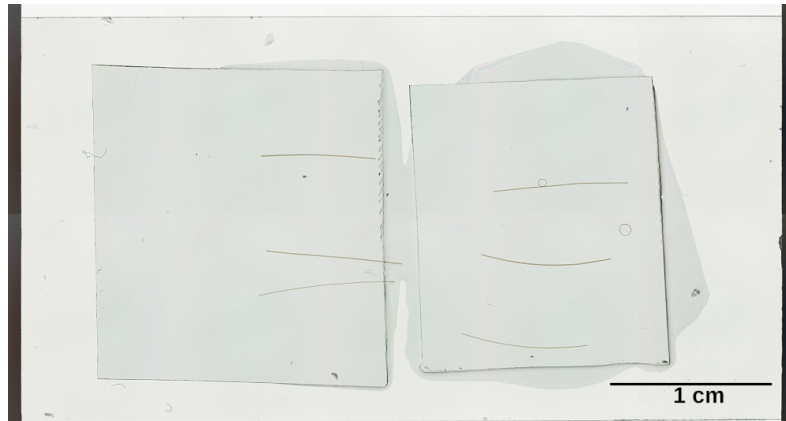


Figure 7: Example of slide mounted with 6 hairs.

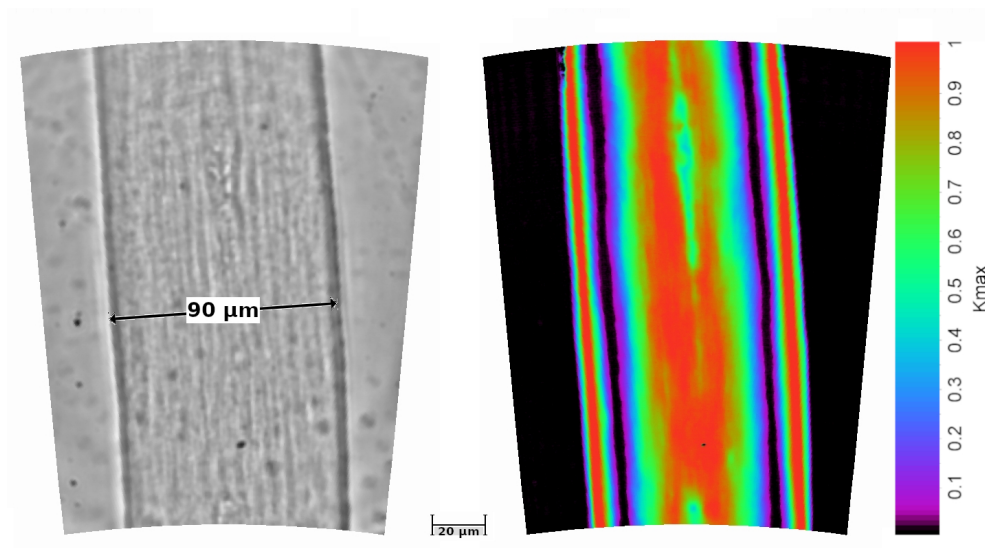


Figure 8: Example of XPolar measurement on a hair. Left: intensity image. Right: K_{max} parameter.

In order to be able to deduce the **birefringence** value from the K_{\max} image, we generated a lookup table: assuming that the hair has a cylindrical geometry, we have simulated the various K_{\max} images that one would obtain on hairs with various diameters and **birefringence**. Thus, if one know the hair diameter (that can be estimated from the intensity image), he can estimate its **birefringence** from the K_{\max} image.

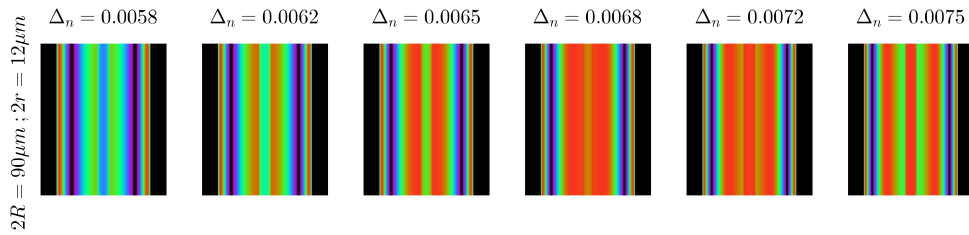


Figure 9: Sample of the lookup table which allows to link a K_{\max} image to a **birefringence** value.

A sample of the lookup table is displayed in Fig. 9, for a hair with a 90 μm diameter, and a 12 μm diameter medulla. To estimate the **birefringence** of the hair in Fig. 8, we compare the image at the right with the images of the lookup table (Fig. 9): we find a **birefringence** Δ_n of 0.0065 ± 0.0003 . That measurement is repeated for all images of all samples, and the results are displayed in Fig. 10, and summarized in Tab. 2. We notice that the oxidation leads to a decrease of 15 % of the mean **birefringence** compared to the value measured on the control sample, with a 10 % statistical significance. However, the active used to protect the hair has limited that decrease at a value of 2 %, with a 6 % statistical significance. In order to increase the significance (i.e. to obtain a p-value $\leq 1\%$), one can increase the population of hair measured (here only 6 per sample) and / or increase the severity of the hair oxidation.

Table 2: Mean value (μ) and standard deviation (σ) of the birefringences measured on each sample. The relative decrease value is computed with the mean values relatively to the control sample.

Sample	μ ($\cdot 10^{-4}$)	σ ($\cdot 10^{-4}$)	Rel. decrease (%)
CTRL	77.9	22.4	NA
E1	65.9	13.9	15
E2	76.3	18.0	2

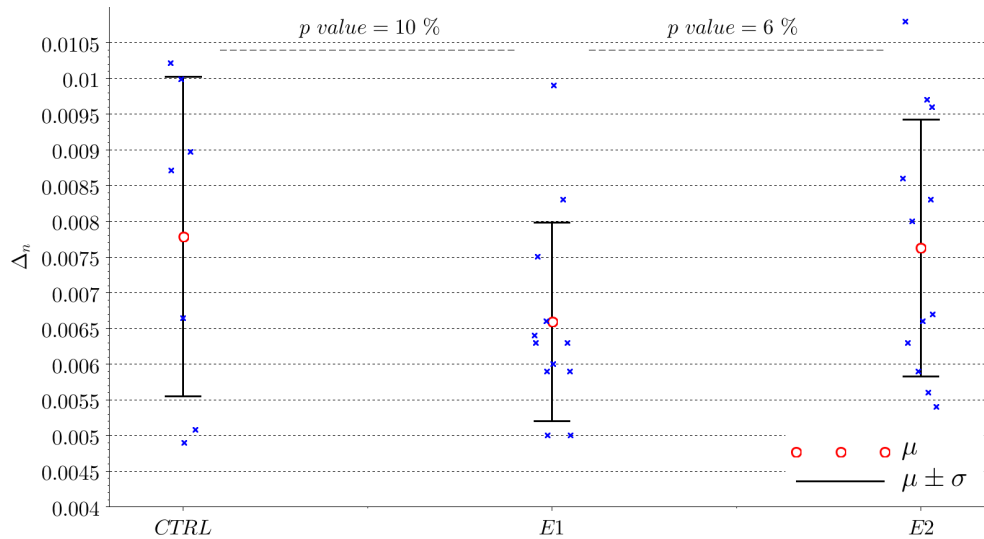


Figure 10: Plot of the birefringences measured on each hair of each sample (blue crosses), mean value (red dots) and ± 1 standard deviation (black lines).

4.3 Conclusion

We have demonstrated that the XPolar technology is sensitive to the condition of the crystalline structure of the hair keratin, here through the oxidation of its disulfide bridges. Indeed, the hair oxidation with hydrogen peroxide has decreased the mean **birefringence** of 15 %. However, the active product used to avoid that decrease has proven its efficiency as the **birefringence** decrease is only 2 % compared to its value without oxidation.

Experimentally, other degradation or protection / care processes of keratin lead to a measurable variation of the hair **birefringence**: for example the use of some oils, high temperatures, natural degradation (ends of hair).

5 GLOSSARY

Here is a didactic glossary intended to facilitate the understanding of the XPolar technology.

5.1 Anisotropy

Anisotropy (the contrary of isotropy) describes the fact that a parameter value is depending on the considered direction. For example, wood has a different tensile strength depending on the fibers direction, or the thermal expansion of crystalline materials that is not the

same along all directions.

Here, we focus on the anisotropy of the materials **refractive index**: depending on the **polarization** direction of light, the **refractive index** of the material will not be the same, and as a consequence the speed of light in the material will not be the same. Such material is described by a property called **birefringence**, and it is able to modify the **polarization** direction of light passing through it.

5.2 Birefringence

Birefringent materials have an anisotropic **refractive index**: its value depends on the **polarization** direction of the incident light.

For the case of uniaxial birefringent materials (most of the natural birefringent materials), there is one direction of propagation for which the material appears to be isotopic (non birefringent). That direction is called optic axis of the material.

for all others propagation directions, the **refractive index** values seen by the light polarized along two perpendicular directions (for example x and y) will vary between two extreme values called ordinary index n_o and extraordinary index n_e . The material birefringence is the value $\Delta_n = n_e - n_o$.

Thus, there are two **polarization** directions for which the material **refractive index** is equal to the extreme values, these directions are called eigen axis. The axis which has the lower **refractive index** is called fast axis, the axis which has the higher **refractive index** is called slow axis. Depending on the fast axis direction in the object plane of a microscope, the intensity of the image seen between **crossed polarizers** will vary, which is a limitation for quantitative applications.

The crossing of a material of thickness e and birefringence Δ_n by a polarized **wave** leads to a maximal phase shift (depending on the **polarization** direction relatively to the material eigen axis) between its orthogonal projections equal to:

$$\theta = \frac{2\pi e \Delta_n}{\lambda}$$

XPolar technology has the property to be insensitive to a rotation in the object plane of the eigen axis, i.e. if the optic axis of the material is contained in the object plane, the measurement result will always be equal to the value described above, for all values of sample rotation. This allows to study samples in a quantitative manner using **polariza-**

tion.

The parameter θ is impacting the equation of the [polarization](#) ellipse: birefringent materials can modify the [state of polarization](#) of an incident light.

5.3 Crossed polarizers microscopy

Microscopy between crossed polarizers consists in illuminating the sample with a white light polarized along a given [state of polarization](#), and to detect the light polarized along the perpendicular direction after having crossed the sample.

Depending on the sample [birefringence](#), it will appear with different colors and light intensity. The apparent color and the [birefringence](#) can be linked with the Michel-Levy chart, however that method does not allow a precise [birefringence](#) measurement.

The company Kamax innovative system commercializes the K-probe silver version, which can in particular produce images between crossed polarizers ; and the K-probe gold version, which includes the XPolar technology allowing the quantitative measurement of the [birefringence](#).

5.4 Electromagnetic wave

The electromagnetic wave is a representation describing electromagnetic radiations. It is propagating in space without requiring material support and carrying electromagnetic radiant energy. It describes the spatial and temporal oscillations of the electric and magnetic fields, both being linked by Maxwell equations. To simplify, we can represent a wave only through one of these fields, the electric field.

Electric field is described by a vector quantity, \vec{E} , which direction is described by its [state of polarization](#).

5.5 K_{\max}

Light parameter measured by XPolar technology.

Let us consider a birefringent sample mounted on a microscopy slide which reflects the light intensity crossing the sample, the collected intensity has thus crossed the sample twice. The incident intensity is polarized along a [polarization state](#) S_k . Two intensities are

measured: I_{\parallel}^k (resp. I_{\perp}^k) by projection of the collected intensity on the **state of polarization** parallel (resp. perpendicular) to the state S_k .

That measurement is repeated for a large number (N) of distinct incident **polarization states**. The K_{\max} value is then obtained with:

$$K_{\max} = \max_{k=1:N} \left\{ \frac{I_{\perp}^k}{I_{\parallel}^k + I_{\perp}^k} \right\}$$

it is linked to the sample **birefringence** through the relation:

$$\begin{aligned} K_{\max} &= \sin^2 \left(\frac{\theta}{2} \right) \\ &= \sin^2 \left(\frac{2\pi e \Delta_n}{\lambda} \right), \end{aligned}$$

with θ the phase shift produced by the **birefringence** Δ_n of the sample of thickness e , for the **wavelength** λ .

5.6 Polarimetry

Polarimetry (ellipsometry) describes the measurement of the **state of polarization** of light. XPolar technology describes a polarimeter able to give information on the sample **birefringence**.

5.7 Refractive index

The refractive index n of a material is an adimensional quantity characterizing the propagation speed v of the **wave** in the material:

$$n = \frac{c}{v}$$

with $c = 3.10^8$ m/s the speed of light in vacuum.

That description is valid only for homogeneous materials, i.e. with a refractive index constant for all directions of **polarization** of light. However, some materials have a refractive index which is different depending on the **state of polarization** of the incident **wave**: depending on its **polarization** direction, the incident **wave** will propagate more or less slowly in the material. Such materials are birefringent, they can modify the **state of polarization** of the incident **wave**.

5.8 State of polarization

The state of polarization of a **wave** represents the direction along which its electric field oscillate during time / propagation.

The amplitude of the electric field $\vec{E}(z, t)$ of a monochromatic plane wave propagating in free space along the z axis is:

$$\vec{E}(z, t) = \begin{bmatrix} E_x(z, t) = E_{0x} \cdot \cos(\omega t - kz + \delta_x) \\ E_y(z, t) = E_{0y} \cdot \cos(\omega t - kz + \delta_y) \\ 0 \end{bmatrix} \quad (1)$$

with $\omega = 2\pi c/\lambda$ the angular frequency of the wave in vacuum, $k = 2\pi/\lambda$ the wavenumber, δ_x and δ_y the phases of the sin waves projected respectively on the x and y axes.

We define $\theta = \delta_y - \delta_x$ the phase shift between the two orthogonal projections of the wave. From the equation above, one can demonstrate that we obtain the equation of an ellipse [1], describing all the directions taken by the vector "electric field" during its propagation:

$$\frac{E_x(z, t)^2}{E_{0x}^2} + \frac{E_y(z, t)^2}{E_{0y}^2} - \frac{2E_x(z, t)E_y(z, t)}{E_{0x}E_{0y}} \cos(\theta) = \sin^2(\theta),$$

with:

- $E_x(z, t)$ (resp. $E_y(z, t)$) the amplitude of the electric field projected on the x axis (resp. y),
- E_{0x} (resp. E_{0y}) the peak amplitude on the x axis (resp. y),
- θ the phase shift between the two sinus $E_x(z, t)$ and $E_y(z, t)$.

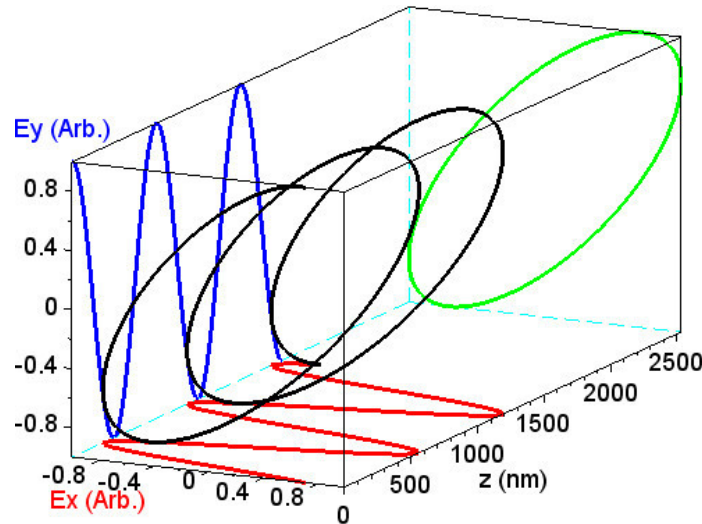


Figure 11: Electric field amplitude $\vec{E}(z, t)$ for an example of plane monochromatic wave (black), $E_x(z, t)$ (red), $E_y(z, t)$ (blue), state of polarization (green).

That ellipse is the state of polarization of the wave. Birefringent materials have the ability to modify the phase shift value θ between

the two cosines $E_x(z, t)$ and $E_y(z, t)$, thus they can modify the state of polarization of the light passing through them.

The XPolar technology allows to probe the sample with all possible states of polarization.

5.9 Wavelength

One of the main parameters describing an [electromagnetic wave](#) is its wavelength, λ , in metric unit. This parameter describes the distance between two consecutive maximums of the [wave](#) amplitude. Visible light is described by waves which wavelength is between 400 and 800 nm.

The wavelength is linked to the frequency ν (Hz) of the [wave](#) by the propagation speed v (m/s):

$$\lambda = \frac{v}{\nu}$$

The propagation speed v of the [wave](#) depends on the [refractive index](#) n of the material in which the [wave](#) is propagating. In vacuum ($n = 1$), the propagation speed is approximately $3 \cdot 10^8$ m/s, the frequencies of visible light are (in vacuum) between 375 THz and 750 THz.

REFERENCES

- [1] D. Goldstein, *Polarized Light*. CRC Press, 2017.
- [2] P. Kraft, C. Evangelista, M. Dacke, T. Labhart, and M. V. Srinivasan, "Honeybee navigation: following routes using polarized-light cues," *Philos. transactions Royal Soc. Lond. Ser. B, Biol. sciences*, vol. 366, no. 1565, pp. 703–708, 2011.
- [3] T. Labhart, "Polarization-sensitive interneurons in the optic lobe of the desert ant *cataglyphis bicolor*," *Die Naturwissenschaften*, vol. 87, pp. 133–6, 2000.
- [4] N. W. Roberts, T.-H. Chiou, N. J. Marshall, and T. W. Cronin, "A biological quarter-wave retarder with excellent achromaticity in the visible wavelength region," *Nat. Photonics*, vol. 3, no. 11, pp. 641–644, 2009.
- [5] T. Cronin, T.-H. Chiou, R. Caldwell, N. Roberts, and J. Marshall, "Polarization signals in mantis shrimps," *Proc. SPIE*, vol. 7461, 2009.

- [6] P. Brady and M. Cummings, "Differential response to circularly polarized light by the jewel scarab beetle *chrysina gloriosa*," *The Am. Nat.*, vol. 175, no. 5, pp. 614–620, 2010.
- [7] M. Blahó, Ádám Egri, R. Hegedüs, J. Jósmai, M. Tóth, K. Kertész, L. P. Biró, G. Kriska, and G. Horváth, "No evidence for behavioral responses to circularly polarized light in four scarab beetle species with circularly polarizing exocuticle," *Physiol. & Behav.*, vol. 105, no. 4, pp. 1067 – 1075, 2012.
- [8] T. W. Cronin, N. Shashar, R. L. Caldwell, J. Marshall, A. G. Cheroske, and T.-H. Chiou, "Polarization Vision and Its Role in Biological Signaling¹," *Integr. Comp. Biol.*, vol. 43, no. 4, pp. 549–558, 2003.
- [9] J. Desroches, D. Pagnoux, F. Louradour, and A. Barthélémy, "Fiber-optic device for endoscopic polarization imaging," *Opt. Lett.*, vol. 34, no. 21, pp. 3409–3411, 2009.
- [10] R. Lattouf, R. Younes, D. Lutomski, N. Naaman, G. Godeau, K. Senni, and S. Changotade, "Picrosirius red staining: A useful tool to appraise collagen networks in normal and pathological tissues," *J. Histochem. & Cytochem.*, vol. 62, no. 10, pp. 751–758, 2014.
- [11] L. Peno-Mazzarino, J. Desroches, G. Percoco, U. Faradova, K. Laquerriere, S. Scalvino, C. Fays, T. Judith, and E. Lati, "The k-probe imaging system as a new tool to analyze human skin aging," *COMET*, 2019.
- [12] C. Miki Hayashi, R. Nagai, K. Miyazaki, F. Hayase, T. Araki, T. Ono, and S. Horiuchi, "Conversion of amadori products of the maillard reaction to ne-(carboxymethyl)lysine by short-term heating: Possible detection of artifacts by immunohistochemistry," *Lab. Investig.*, vol. 82, no. 6, pp. 795–808, 2002.
- [13] P. Gasser, F. Arnold, L. Peno-Mazzarino, D. Bouzoud, M. T. Luu, E. Lati, and M. Mercier, "Glycation induction and antiglycation activity of skin care ingredients on living human skin explants," *Int. J. Cosmet. Sci.*, vol. 33, no. 4, pp. 366–370, 2011.
- [14] P. J. Thornalley, "Use of aminoguanidine (pimagedine) to prevent the formation of advanced glycation endproducts," *Arch. Biochem. Biophys.*, vol. 419, no. 1, pp. 31 – 40, 2003.
- [15] M. Feughelman, *Mechanical properties and structure of alpha-keratin fibres : wool, human hair, and related fibres*. Sydney: UNSW Press, 1997.

- [16] R. Fraser, T. MacRae, L. Sparrow, and D. Parry, "Disulphide bonding in α -keratin," *Int. J. Biol. Macromol.*, vol. 10, no. 2, pp. 106–112, 1988.
- [17] A. J. Grosvenor, S. Deb-Choudhury, P. G. Middlewood, A. Thomas, E. Lee, J. A. Vernon, J. L. Woods, C. Taylor, F. I. Bell, and S. Clerens, "The physical and chemical disruption of human hair after bleaching – studies by transmission electron microscopy and redox proteomics," *Int. J. Cosmet. Sci.*, vol. 40, no. 6, pp. 536–548, 2018.